# ACOUSTIC BUBBLE SIZING: FROM THE LABORATORY TO SURF ZONE TRIALS

Timothy G Leighton MIOA, Andy D Phelps & David G Ramble

## Introduction

The ability to detect bubbles has a range of industrial, medical and environmental applications [1]. Historically interest concentrated on characterising violent cavitation and its effects (eg erosive [2], biological [3] and chemical [4]), brought about when the local pressure around a small bubble nucleus changes in such a way as to bring about sudden bubble growth, followed by a rapid collapse. Reasons for detection of stable bubbles have progressed from a need to characterise the nuclei in order to predict the likelihood of cavitation, to an understanding of the importance of such stable bubbles in their own right. This includes monitoring the near-surface oceanic bubble population to gain information of the atmosphere/ocean transfer of momentum and mass [5].

There is a wide range of techniques which can characterise cavitation [6] and stable bubbles [7]. Acoustic techniques have many advantages, including the abilities to directly infer the size of the bubbles and discriminate between gas and solid particles. However, all techniques individually have limitations. This report starts with a description of the different techniques, illustrated with experimental results taken in the laboratory, and discusses how their individual advantages and limitations may be exploited to best effect. Following this, one of these techniques is exploited in a preliminary deployment in the surf zone to measure the oceanic population.

## Laboratory Study: A Comparison of Acoustic Techniques

The combined use of several acoustic techniques not only reveals, and to some extent compensates for, the limitations of each [8], but also might be used to give additional information. An example of this is a comparison of the bubble population measured through 'active' techniques with that obtained from the passive emissions which are excited from bubbles when they are entrained. Since the passive emissions decay over millisecond timescales, they reflect the population characteristics at the time of entrainment (eg by a breaking wave). Active techniques must be used to measure the population at a later time. A comparison of these two estimates might yield information on the way dissolution, buoyancy and liquid flow can remove bubble gas from the population, and so may be relevant to the atmosphere/ocean transfer studies outlined above. An experimental comparison of these acoustic techniques has been the focus of recent work, and a description of the apparatus and calibration is given elsewhere [8]. In this article each of the signals will be introduced and the advantages and disadvantages of its application to in situ bubble sizing discussed.

A pulsating gas bubble in a liquid is a lightly-damped oscillator, the stiffness being invested in the gas and the inertia in the surrounding liquid [1]. As such, if an air bubble (roughly resembling a sphere of radius $R_0$) is injected into water at around atmospheric pressure, a nearby hydrophone will detect an acoustic pressure fluctuation resembling an exponentially decaying sinusoid at the natural frequency $\nu_0 \approx 3.3/R_0$ (using SI units). The detected frequency gives the bubble size (Figure 1a). A few milliseconds later, these passive emissions have effectively ceased, and as the bubble rises under buoyancy it must be detected by an active technique. The bubble can be sized from its resonance, found for example through the scattering of a 'pump' signal, which may be broadband, a chirp, or a sequence of tones at a pump frequency of $\omega_p/2\pi$ Hz. The closer the pump signal comes to exciting a bubble at its resonance, the greater the pulsation amplitude and the more strongly it backscatters the insonifying signal. However, strong scattering at a particular frequency might also be obtained from a bubble which is much larger than resonance size, which though it does not pulsate significantly, presents to the incident field a large target [7]. Although this represents an ambiguity when using the signal as an indicator of resonant bubbles, such geometrical scattering can be exploited by insonifying the bubble with an ultrasonic beam whose frequency is much higher than the bubble resonance. This is demonstrated in Figure 1b, and typical results taken using a 3.5 MHz clinical diagnostic scanner are presented in Figure 2.

However, the bubble is a nonlinear oscillator (the stiffness is nonlinear [1], and the wall motion must clearly be asymmetric since it can theoretically expand without limit, but cannot contract beyond zero radius). This nonlinear behaviour is demonstrated in the sequence of pictures given in Figure 3, where an air bubble in glycerol is being driven at its resonance frequency of 100 Hz, and its volume is clearly not simply varying sinusoidally about equilibrium. In general, as the pump frequency approaches a bubble resonance, the amplitude of oscillation of the bubble wall becomes greater, and these nonlinear characteristics become more manifest: the resonant bubble generates harmonics, subharmonics, and ultraharmonics at $2\omega_p$, $3\omega_p$ ...; $\omega_p/2$; and $3\omega_p/2$, $5\omega_p/2$ etc. Therefore, though when the pump signal is far from the bubble resonance, the detected signal should contain only the transmitted frequency $\omega_p$; when it approaches the bubble resonance, one expects a harmonic spectrum about $\omega_p$ (Figure 1c). To be an unambiguous indicator of bubble size, these spectral components must be excited only when the pump frequency is close to the bubble resonance. The off-resonance fall off of these various signals

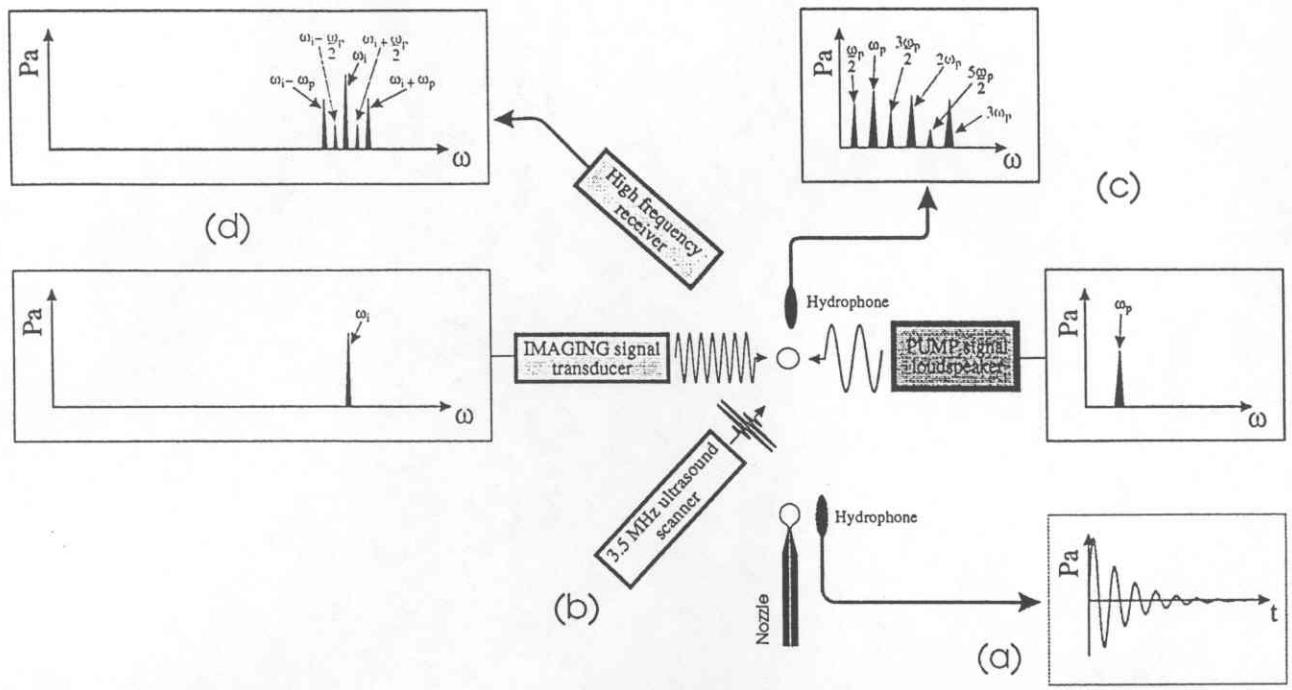


Fig. 1. Schematic of the apparatus required to implement the various acoustic detection techniques, a simultaneous deployment of which has been realised [8]. In (a) the bubble is shown, injected from a nozzle, where a hydrophone detects its short duration passive emissions. In contrast, all the active techniques are schematically shown interrogating a bubble which has risen under buoyancy. In (b) a medical diagnostic ultrasound scanner is deployed to produce an image of the bubble (shown in Figure 2). In (c) the underwater loudspeaker generates a series of tonal pump signals, and a second hydrophone detects structure in the spectrum corresponding to $2\omega_p$, $3\omega_p$, $\omega_p/2$, $3\omega_p/2$ and $5\omega_p/2$ in the presence of a resonant bubble. In (d) a high frequency imaging signal is projected onto the bubble, and the scattered signal is detected by a high frequency receiver. Whilst in the absence of the bubble, ideally only $\omega_p$ and $\omega_i$ can be should be present, a resonant bubble will produce structure in the spectrum around $\omega_i$. The various peaks have been colour coded to facilitate their identification in later results (Figs. 4, 5 and 10)

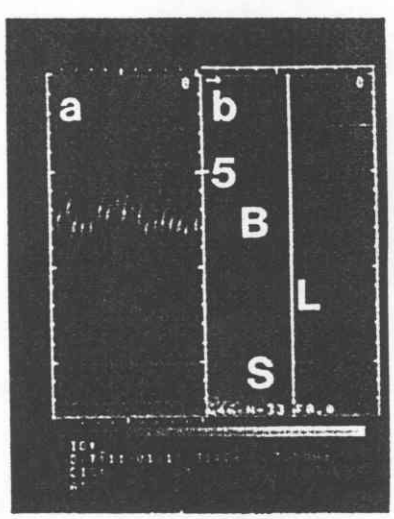


Fig. 2. This output shows both the a) M- and b) B-mode images obtained using a medical ultrasound scanner, the section shown being a slice at 45° to vertical [8].
Bubbles, rising under buoyancy, pass through the beam section. The bubble (labelled B) can be located in Fig. 2b (near-field is at top of image), which also images the underwater loudspeaker (S). Images which intersect the vertical line (L) in 1 s are plotted in Fig. 2a: almost 19 bubbles pass through the beam in that time, with rise speed (from the image, assuming local rectilinear bubble motion in the 45° beam orientation) of 20 ± 2 cm/s, covering an implied 0.87 – 1.13 mm radii range [8]

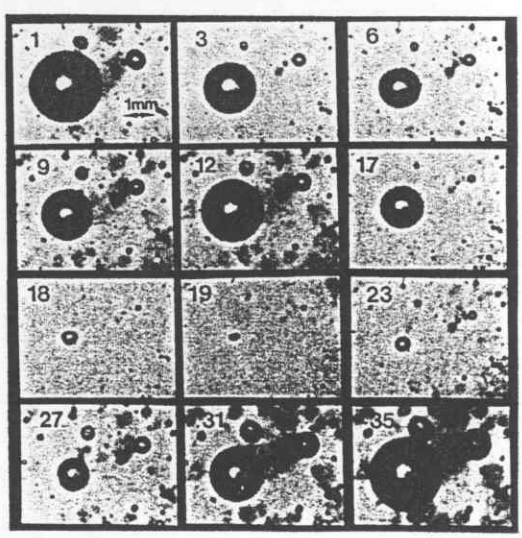


Fig. 3. Selected frames taken from a sequence of photographs of a 100 Hz air bubble in glycerol being driven at its resonance frequency, with a pump amplitude of 3900 Pa. The 35 frame sequence contains the periodic repeating cycle of oscillation, and the figure shows selected frames from this sequence. They show the bubble contracting from a maximum size in frame 1 to a minimum in frame 6, expanding to a second maximum (frame 12), then collapsing to a second minimum (frame 19) before expanding to the initial size. The second collapse is gradual up to frame 17, but then becomes very rapid.

can be seen from Figure 4a, where a single bubble resonant at 1950 Hz was tethered to a horizontal wire and was then insonified at discrete tones from $\omega_p/2\pi$ = 1700 Hz to 2200 Hz in 25 Hz steps. The harmonically related signals at $2\omega_p$ and $3\omega_p$ are excited off-resonance, and in fact are excited when no bubble is present (Figure 4b) as a result of nonlinear processes in the apparatus and propagation through the water. The non-integer harmonic signals at $\omega_p/2$, $3\omega_p/2$ and $5\omega_p/2$ initially appear to be better indicators of the bubble presence and resonance. However, these signals do not propagate well into the medium, as the nonlinearities do not arise from monopole volumetric pulsations in the bubble motion. For example, the subharmonic oscillation at $\omega_p/2$ (at the low pump signal amplitudes required to be minimally invasive [9]) is generated only when the pump signal amplitude exceeds the threshold required to excite Faraday waves on the bubble wall [10], and the pressur fluctuations resulting from such oscillations do not propagate to distance.

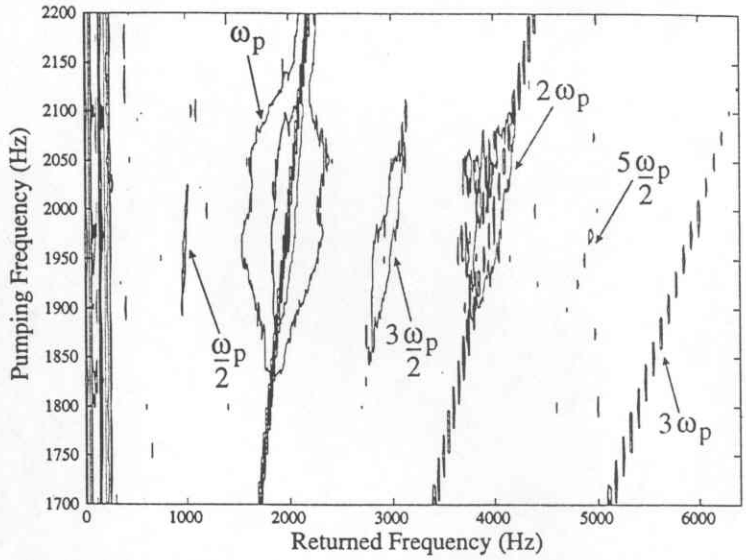


Fig. 4a. Contour plot showing the through resonance response for a 1950 Hz resonant bubble, tethered to a horizontal wire at a distance of approximately 1 mm from the active element of a hydrophone to allow any non-monopole bubble emissions to be detected. The frequency step size was 25 Hz and the insonification amplitude was 150 Pa (0 – pk).

Many of these drawbacks can be overcome with the use of a combination frequency technique [11]. With this technique the bubble is driven at its resonance using the pump signal described earlier, and simultaneously with an 'imaging' signal at a much higher frequency $\omega_i$, typically of the order of a few MHz (Figure 1d). The scattered high frequency sound from the bubble is then detected by a high-frequency receiver. Consider a bubble which is only pulsating volumetrically (ie without surface waves). The strength of the target which the bubble presents to the imaging beam varies periodically as the bubble pulsates, and so the scattered imaging beam is amplitude modulated by the bubble, generating frequency sidebands at $\omega_i \pm \omega_p$. The further the pump frequency is from resonance, the smaller the displacement amplitude of the pulsation, so that the energy invested in these sidebands is reduced. Thus the technique allows the exploitation of the first-order resonant behaviour of a bubble, but without the ambiguity caused when a large bubble can be mistaken for a small resonant bubble. Additionally, the use of combination frequency measurements allows very specific spatial localisation of the bubble, and the process translates only bubble mediated information from the noisy frequency window around their resonance up to the comparatively quieter frequency window around the imaging signal.

Although any bubble wall effects which do not give rise to a volumetric pulsation do not themselves produce acoustic signals which propagate to distance in the medium, they too can be used to modulate the imaging beam, which does propagate. In the case of the subharmonic oscillation generated by Faraday waves on the bubble wall at half the driving frequency, these provide a modulation of the acoustic cross-sectional target area presented to the high frequency signal, and this manifests itself in the returned frequency plots as signals at $\omega_i \pm \omega_p/2$ [12].

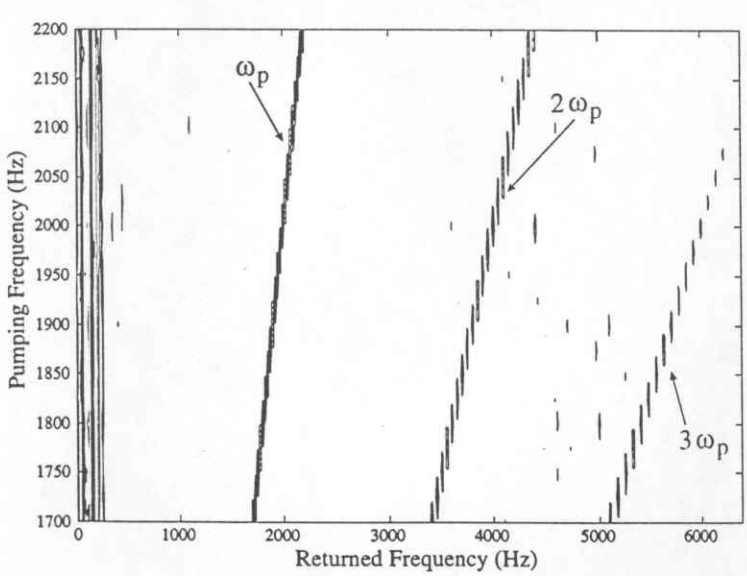


Fig. 4b. Experiment repeated in the absence of a bubble

These combination frequency signals are demonstrated in the data shown in Figure 5. A uniform stream of bubbles was injected to rise through the common focus of the high frequency transmitter and receiver transducers. The imaging sound field was set at a constant 1.135 MHz, and the pump sound field incremented from 2500 Hz to 3500 Hz in 25 Hz steps, at a pressure amplitude of 160 Pa (0-pk). The returned signal from the high frequency receiver was then heterodyned before data acquisition: this procedure involves multiplying the analogue signal returned from the high frequency preamplifier with a second signal

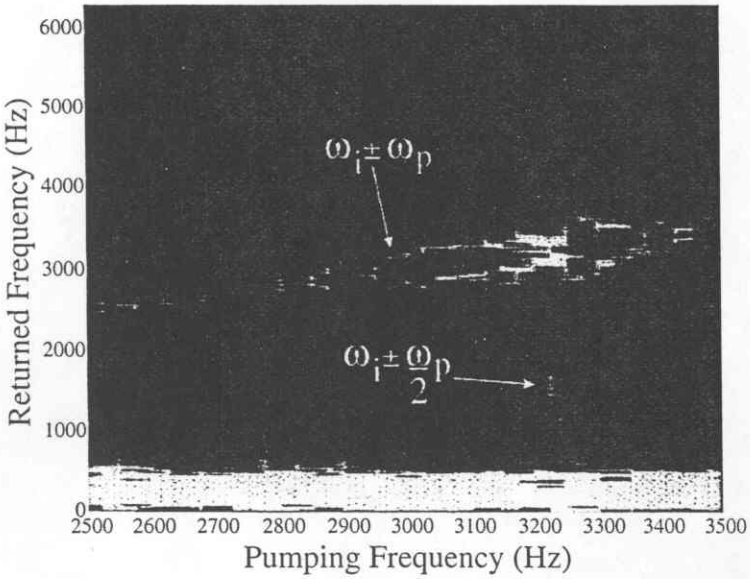


Fig. 5. Grey-scale map of the returned signal strength through resonance for bubbles of one size rising through the focus of the two high frequency transducers in the combination frequency tests. The bubbles were insonified at 160 Pa (0 – pk), and the pumping frequency was incremented in 25 Hz steps.

from the imaging frequency signal generator. As a result the useful information contained just above the imaging frequency is reproduced at just above dc, and the information just below the imaging frequency is also reproduced above dc but in anti-phase. This enables much lower sampling rates and data storage.

At each setting of the pump frequency, the returned signal was heterodyned and the spectrum obtained. These spectra are illustrated as a grey-scale plot over the range of pump frequencies used. In the plot, the signals at $\omega_i \pm \omega_p$ and $\omega_i \pm \omega_p/2$ are clearly visible. As expected, though the signal at $\omega_i \pm \omega_p$ reaches a maximum value at the bubble resonance, the off-resonance pulsation causes it to extend over a wide frequency range. Clear confirmation that the resonance of the bubbles in the stream occurs at a pump frequency setting of 3225 Hz is given when structure in the heterodyned spectrum at the subharmonic of the driving frequency is also evident. Each of the heterodyned $\omega_i \pm \omega_p$ and $\omega_i \pm \omega_p/2$ signals, where they occur, are themselves separated into their two peaks, corresponding to $\omega_i+\omega_p$ and $\omega_i-\omega_p$, and to $\omega_i + \omega_p/2$ and $\omega_i - \omega_p/2$, respectively. After heterodyning, the difference information is reproduced overlaid on the sum information, but owing to the Doppler shift from the moving bubbles the centre frequency of the returned signal is no longer exactly at the imaging frequency.

## Discussion on the Laboratory Tests

The laboratory tests indicate that if only one driving frequency ($\omega_p$) is employed to characterise a single bubble, the clearest indication of the bubble resonance, and therefore its size, is given by the presence of non-integer harmonics of the driving sound field, and especially a subharmonic at $\omega_p/2$. However, these signals are caused by surface phenomena and do not propagate into the medium. This limitation is overcome through the use of a combination frequency insonification technique, which results in emissions at frequencies of $\omega_i \pm \omega_p/2$ as well as at $\omega_i \pm \omega_p$. It has been demonstrated [12,13], however, that although the combination frequency signal involving the subharmonic of the driving sound field can give an accurate and unambiguous indicator of a resonant bubble, it is a particularly difficult emission to stimulate and analyse. Because the Faraday waves on the bubble surface are parametric in nature, it is necessary to drive the bubbles at exactly the right amplitude to maximise the accuracy of the technique – too low and the signal will not be stimulated, too high and the pump frequency span over which the emission occurs increases and much of the accuracy benefit is lost. To date in experiments, the amplitude of the signal scattered at $\omega_i \pm \omega_p/2$ from a single bubble has not been sufficiently reproducible to warrant relating the amplitude to the number of bubbles in a population resonant at that frequency [14]: reliable counting can only be achieved if no two bubbles are so close as emit $\omega_i \pm \omega_p/2$ signals at any given pump frequency. Additionally, the surface waves themselves are very lightly damped, so that ideally a period of insonification before the data are collected is required to allow for any transient effects to decay. The signal at $\omega_i \pm \omega_p$, however, is attributable to the volumetric pulsations of the bubble, and therefore behaves much more predictably. At present the $\omega_i \pm \omega_p/2$ signal content can unambiguously detect a resonance whilst simultaneous observation of the $\omega_i \pm \omega_p$ signal could give the bubble count [8]. In this test study the oceanic data concentrated on analysing these $\omega_i \pm \omega_p$ signals. Although these combination frequency com-

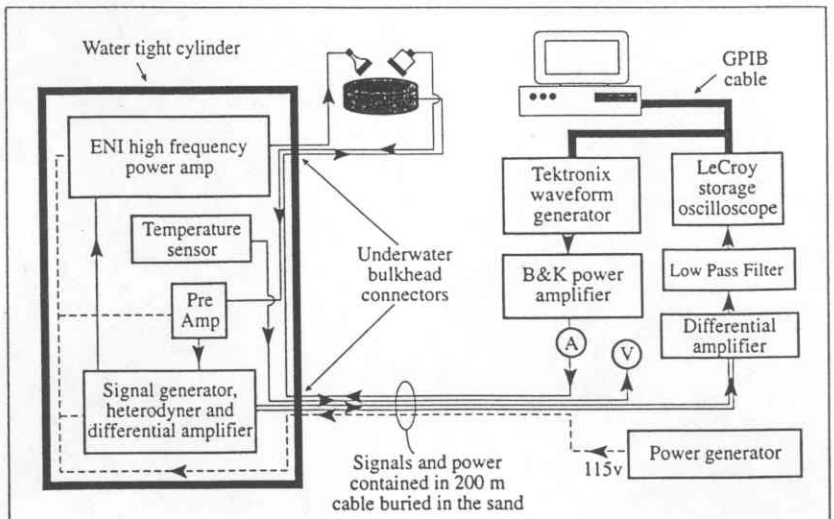


Fig. 6. Schematic of the apparatus used in the oceanic measurements

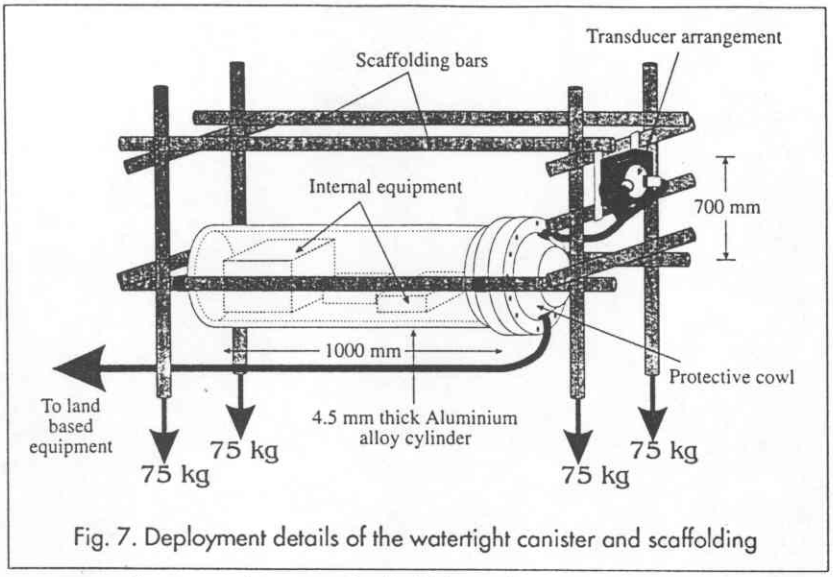


Fig. 7. Deployment details of the watertight canister and scaffolding

ponents will occur whenever the bubble pulsates, and so can be detected far from resonance, the $\omega_i \pm \omega_p$ signals reach a maximum amplitude when the pump sound field becomes coincident with a bubble resonance, and thus can be used to get a statistical measure of the oceanic population.

## Oceanic Data Collection

Oceanic tests were performed in the North Sea between 26th and 30th November 1995, on a beach in Tunstall in East Yorkshire. The aim was to measure the bubble population at a point in the shallow water surf zone. This was performed in tandem with sonar measurements of the surf zone bubble cloud profiles taken by the Southampton Oceanography Department. The beach was chosen because of its slight gradient, which allowed the equipment to be set up at low tide and anchored to the sand, such that as the tide came in it would eventually cover the rig enabling measurements to be taken. The data collection was performed at four spot frequencies: 28 kHz, 50 kHz, 60 kHz and 88 kHz. This was so that the data could be directly compared with earlier oceanic bubble measurements [15] which relied on measuring the direct acoustic backscatter from individual sonar transducers. The current tests used a 3 kPa pump signal amplitude, and 25 four frequency samples were taken over a 3.5 minute period every half hour that the transducers were immersed. As the signals were broadcast consecutively with no gap, each measurement lasted only 0.4 s.

The equipment set up used in the sea trials is shown in the schematic in Figure 6, and a complete description of the apparatus and calibration techniques can be found elsewhere [16]. The figure shows a remote equipment canister which was placed in the sea, containing a high frequency power amplifier, the imaging signal generator and heterodyner equipment, the returned signal preamplifier, and a temperature sensor to ensure that the equipment did not overheat. The canister comprised a 1000 mm long x 355 mm diameter watertight aluminium alloy cylinder with a shell thickness of 4.5 mm, which was painted to minimise corrosion and clamped to a rigid scaffold structure as shown in Figure 7. A photograph of the equipment set-up on the beach at low tide before immersion is included in Figure 8, and a picture of the rig becoming uncovered after the measurements as the tide went out in Figure 9.

A typical spectrum from the sea trials is presented in Figure 10, taken from a 28 kHz insonification. The particular data were collected at 22.30 on the 29th November 1995, when the wind speed was 11 m/s, and the transducers were immersed at a depth of 1.5 m in water approximately 3 m deep. The data shows the heterodyned signal from the high frequency receiver, in which the imaging signal is visible at 1 kHz (not at dc owing to the Doppler shift from the moving bubble targets). The sum frequency spectral information contained just above the imaging signal is also shown, at approximately 29 kHz, and the difference data shown at 27 kHz. Between the two combination frequency peaks is a single spike at 28 kHz. This is caused by the nonlinear combination of the pump and imaging signals by turbulence in the detection zone, and can be therefore distinguished from the actual bubble mediated information.

The data collected over these 25 time intervals were analysed to get the individual heights of the heterodyned sum signals, and time averaged so that comparisons with

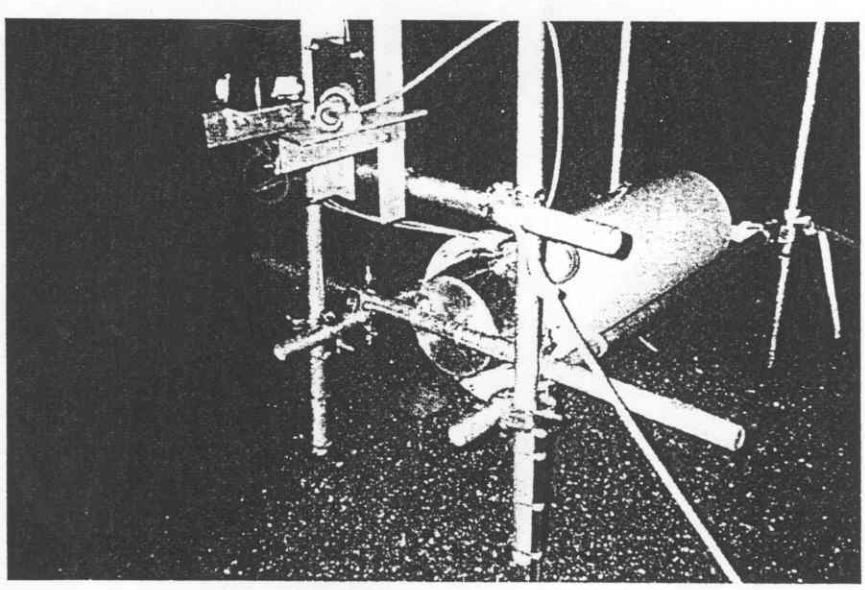

Fig. 8. Photograph of the canister and remote equipment set-up on the beach at low tide, taken at night before the oceanic measurements were taken

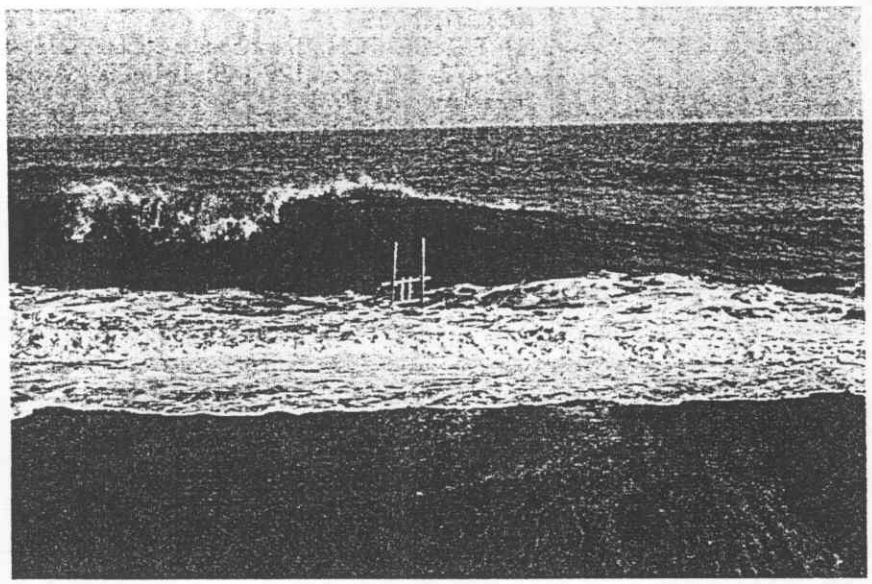

Fig. 9. Photograph of the canister becoming uncovered the morning afterwards with the tide going out

existing bubble data is possible. These data were taken from Farmer and Vagle [15], Breitz and Medwin [17] and Johnson and Cooke [18] who have all previously applied different bubble estimators to measure the oceanic distributions. The traditional method of presenting the data is in numbers of bubbles per $m^3$ per micrometer radius range, and Figure 11 shows the three sets of data superposed with the time averaged population measured using the two frequency technique. The radius range over which these signals existed was numerically calculated from linear theory of the behaviour of a range of bubble radii to the four frequencies employed [1], defined by where the individual contributory sound pressure level was 3 dB down on the maximum resonant level. The effective insonification volume was theoretically estimated as 0.20 $m^3$ by performing a Rayleigh integral over the surface of the two high frequency transducers.

The data shown in Figure 11 show that the bubble population measured using the two-frequency technique exceeds the other estimates over the whole radius range. This is to be expected as the data were collected in the surf zone where, because of the continual wave action, a high concentration of bubbles is created. Farmer and Vagle collected their data in a 12 – 14 m/s wind speed from bubble scatter in a 4 km deep channel using upwards-facing sonar designed to monitor the linear backscatter from the bubble population. Johnson and Cooke used photographic estimates in 20 – 30 m deep water, of which the population estimate at 0.7 m depth and 11 – 13 m/s wind speed is included. Breitz and Medwin collected their oceanic data with a flat plate resonator, which again exploits the linear resonance of bubbles. They measured in water 120 m deep in 12 – 15 m/s wind speeds and at a depth of 25 cm. Thus, although the weather conditions were similar over the four sets of collected data, the local sea dynamics were very different for the Tunstall measurements because of the presence of surging breakers.

## Summary

This article has examined the various signals produced when a gas bubble in water interacts with an insonifying sound field. The geometric scattering from the impedance mismatch at the bubble surface was demonstrated, and the individual signals generated by a resonant bubble were also identified. Then the ability of the combination frequency technique to detect and estimate the resonance frequency of individual bubbles in the laboratory was discussed, and it was demonstrated how this overcame earlier ambiguities and inaccuracies. These combination frequency signals occur when a bubble is insonified at resonance, and a second high frequency sound field is simultaneously applied: the strength of the high frequency signal scattered from the bubble is thereby amplitude modulated as the bubble's acoustic cross-section varies periodically. Two potential combination frequency signals were identified, at $\omega_i \pm \omega_p$ and $\omega_i \pm \omega_p/2$. It was shown that the signals involving the subharmonic stimulated at the bubble's resonance were more accurate and less ambiguous indicators of the

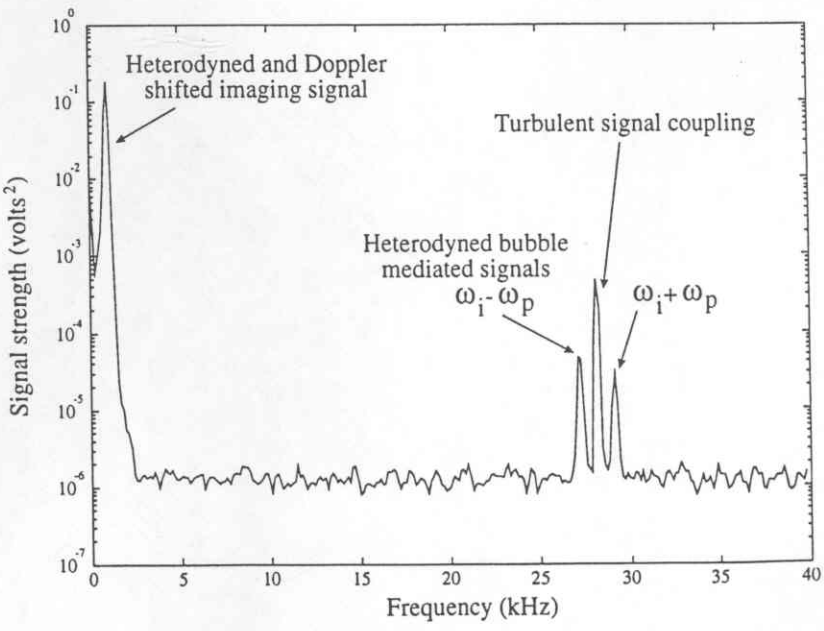


Fig. 10. Typical results from the oceanic tests, showing the heterodyned frequency content for a 28 kHz insonification signal

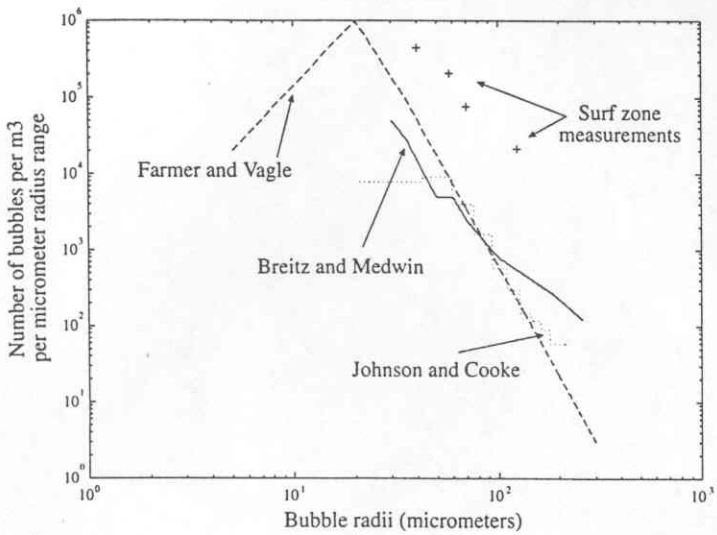


Fig. 11. Comparison of time averaged oceanic data with earlier estimates, taken from Farmer and Vagle [15], Breitz and Medwin [17] and Johnson and Cooke [18]. The associated uncertainties will be discussed in a future paper.

resonance frequency, and this is attributed to the higher order of nonlinearity involved in generating the signals (the subharmonic combination frequency signal at $\omega_i \pm \omega_p/2$ occurs when Faraday waves set up on the bubble surface at half the driving frequency provide a modulation in the target area presented to the imaging sound field). These signals are, however, very difficult to exploit in a potential bubble sizer as they are parametric, the height of their backscattered signal is at present unpredictable, and they
are so lightly damped that before measurement data are taken, insonification over a large number of driving cycles must occur to allow for transients to decay.

As a result, the combination frequency volumetric backscatter at $\omega_i \pm \omega_p$ was used in an oceanic bubble sizing experiment performed in the surf zone on a beach in Yorkshire, England. The results show that ambiguities which affected earlier workers caused by turbulent coupling of the two sound fields can be identified and removed from the analysis, and that the considerable off-resonance signal strength can also be accounted for. The results, when compared against three earlier studies performed in similar wind conditions, show a greater number of bubbles in our measurements, which is caused by the much more dynamic and populated nature of the surf zone.

## Acknowledgements

The authors wish to extend their thanks to David Baldwin, Alan Hall and Prof Steve Thorpe from the SOC for their assistance with the beach tests, and to Rob Stansbridge, John Taylor, Mike Bartlett, Dave Edwards and John Hawkes and the Southampton University Physics Technical Workshop for their help with the design and manufacture of the oceanic rig. The work was carried out using a NERC award (ref. GR3 09992), whilst David Ramble is himself funded by EPSRC (ref. GR/H 79815).

## References

[1] T G LEIGHTON, 'The Acoustic Bubble', 216, 442, 465–472, 542-556; 129-148; 181; 306; Academic Press, London, (1994)
[2] LORD RAYLEIGH, 'On the pressure developed in a liquid during the collapse of a spherical cavity', Phil Mag, 34, 94–98, (1917)
[3] C R HILL (Ed), 'Physical principles of Medical Ultrasonics', John Wiley and Sons, New York, (1986)
[4] K S SUSLICK (Ed), 'Ultrasound: its chemical, physical, and biological effects', VCH Publishers, New York, (1988)
[5] S A THORPE, 'On the clouds of bubbles formed by breaking wind-waves in deep water, and their role in air-sea gas transfer', Philos Trans R Soc London, A, 304, 155–210, (1982)
[6] T G LEIGHTON, 'Acoustic Bubble Detection. II. The detection of transient cavitation', Environmental Engineering, 8, 16–25, (1994)
[7] T G LEIGHTON, 'Acoustic Bubble Detection. I. The detection of stable gas bodies', Environmental Engineering, 7, 9–16, (1994)
[8] T G LEIGHTON, D G RAMBLE & A D PHELPS, 'Comparison of the abilities of multiple acoustic techniques for bubble detection', Proc of the Institute of Acoustics, 17, 149–160, (1995)
[9] T G LEIGHTON, A D PHELPS & D G RAMBLE, 'Bubble detection using low amplitude multiple acoustic techniques', In J S Papadakis (Ed), Proc of the 3rd Conference on Underwater Acoustics, Heraklion, Crete, in press, (1996)
[10] A D PHELPS & T G LEIGHTON, 'The subharmonic oscillations and combination-frequency subharmonic emissions from a resonant bubble: their properties and generation mechanisms', Acta Acustica, in press, (1996)
[11] V L NEWHOUSE & P M SHANKAR, 'Bubble sizing using the nonlinear mixing of two frequencies', JASA, 75, 1473–1477 (1984)
[12] A D PHELPS & T G LEIGHTON, 'High resolution bubble sizing through detection of the subharmonic response with a two frequency excitation technique', JASA, 99, in press, (1996)
[13] A D PHELPS, 'Characterisation of the subharmonic response of a resonant bubble using a two frequency technique', PhD Thesis, University of Southampton, (1995)
[14] A D PHELPS & T G LEIGHTON, 'Investigations into the use of two frequency excitation to accurately determine bubble sizes', In J Blake, J M Boulton-Stone and N H Thomas (Eds), Bubble Dynamics and Interface Phenomena - Proc of an IUTAM symposium held in Birmingham, UK, 6-9 September 1993, 475–484, Kluwer Academic Press, (1994)
[15] D M FARMER & S VAGEL, 'Waveguide propagation of ambient sound in the ocean-surface bubble layer', JASA, 86, 1897–1908, (1989)
[16] A D PHELPS, D G RAMBLE & T G LEIGHTON, 'Characterisation of the oceanic bubble population using a combination frequency technique', In J S Papadakis (Ed), Proc of the 3rd Conference on Underwater Acoustics, Heraklion, Crete, in press, (1996)
[17] N BREITZ & H MEDWIN, 'Instrumentation for in situ acoustical measurements of bubble spectra under breaking waves', JASA, 86, 739–743, (1989)
[18] B D JOHNSON & R C COOKE, 'Bubble populations and spectra in coastal waters; a photographic approach', J Geophys Res, 84, C7, 3761-3766, (1979)

**Timothy G Leighton MIOA, Andy D Phelps and David G Ramble are at the Institute of Sound and Vibration Research, University of Southampton. This article is a modified version of the A B Wood Memorial Lecture given by Dr Leighton in December 1995** ❖